

Fluid-structure interaction algorithm for an elastic structure with large deformations

A. Pecka, O. Bublík

*NTIS – New Technologies for the Information Society, Faculty of Applied Sciences, University of West Bohemia,
Univerzitní 8, 301 00 Plzeň, Czech Republic*

This contribution introduces a fluid-structure interaction (FSI) methodology where the structure is considered elastic. One of the main requirements for the FSI algorithm is a high level of modularity, meaning that the fluid and structure solvers are independent of each other and the meshes do not need to align on the fluid-solid interface. For this reason, a partitioned approach was adopted with the option of either weak or strong coupling.

Compressible Navier-Stokes equations in the arbitrary Lagrangian-Eulerian formulation are considered as the mathematical model for the fluid flow. The fluid dynamics is simulated using an implicit discontinuous Galerkin finite-element scheme with Newton's iterative procedure. The interior penalty method is used to approximate viscous fluxes. The discontinuous Galerkin solver is being developed by the authors of this contribution under the name FlowPro [1]. FlowPro is a multipurpose numerical software that solves system of hyperbolic and parabolic partial differential equations. The elastic structure is described by nonlinear equations of elastodynamics that allow for large deformations. The system is solved by an implicit finite-element scheme with Newton's iterative procedure. The finite-element structure solver is also a product of the authors of this contribution.

Since the fluid and structure meshes are mutually nonconforming on the fluid-solid interface, the aerodynamic stress tensors needs to be interpolated from the fluid mesh to the structure mesh. The interpolation is achieved by radial basis functions. Likewise, the displacement determined by the structure solver needs to be interpolated onto the fluid mesh on the fluid-solid interface. The interpolation is taken care of by the mesh-deformations algorithm, which is also based on radial basis functions.

The FSI algorithm is validated on the well-known Turek-Hron benchmark, which was first proposed in [2] and then again published in [3]. The benchmark consist of three FSI problems with a 2D incompressible laminar flow around a fixed cylinder with elastic cantilever embedded in the cylinder. The vortices that are shed from the cylinder excite oscillations in the cantilever. The geometric parameters are tabulated in Table 1 (left). The no-slip boundary condition is prescribed at the walls - the fixed cylinder, the elastic cantilever and the upper and lower walls. At the inlet on the left-hand side of the fluid domain, a parabolic velocity profile is prescribed as ${}^f v_{in}(y) = 35.69 {}^f \bar{v}_{in} y ({}^f H - y)$ with mean inlet velocity ${}^f \bar{v}_{in}$. The outlet pressure is chosen such that the free-stream Mach number is 0.05 and thus the flow can be considered incompressible. The reason for the choice of an incompressible-flow benchmark for the compressible-flow solver is the lack of benchmarks for FSI problems.

The structure and fluid parameters found in Table 1 (right) are chosen such that for FSI1 the flow stabilises at the steady state, whereas FSI2 and FSI3 lead to periodic oscillations of

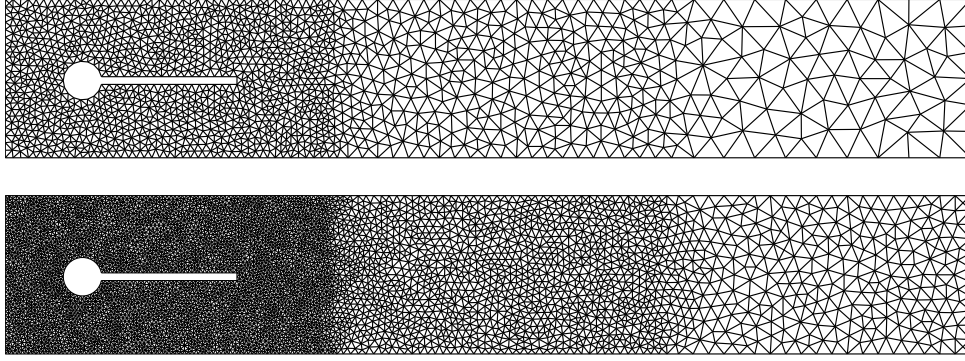


Fig. 1. Coarse mesh with size $h = 0.02$ m and 3040 elements (*top*) and fine mesh with size $h = 0.01$ m and 12 092 elements (*bottom*)

Table 1. Geometric parameters (*left*) and physical parameters (*right*)

	symbol	value [m]	symbol	units	FSI1	FSI2	FSI3
channel length	fL	2.5	${}^s\rho$	$\frac{\text{kg}}{\text{m}^3}$	10^3	10^4	10^3
channel height	fH	0.41	sE	$\frac{\text{kg}}{\text{m s}^2}$	$1.4 \cdot 10^6$	$1.4 \cdot 10^6$	$5.6 \cdot 10^6$
cylinder centre	C	[0.2, 0.2]	${}^s\nu$	$\frac{\text{kg}}{\text{m s}^2}$	0.4	0.4	0.4
cylinder radius	r	0.05	${}^f\rho$	$\frac{\text{kg}}{\text{m}^3}$	10^3	10^3	10^3
cantilever length	sL	0.351 01	${}^f\mu$	$\frac{\text{kg}}{\text{m s}}$	10^{-3}	10^{-3}	10^{-3}
cantilever height	sH	0.02	${}^f\bar{v}_{\text{in}}$	$\frac{\text{m}}{\text{s}}$	0.2	1	2
reference point	A	[0.6, 0.2]	Re	-	20	100	200

the structure at a frequency close to the second lowest natural frequency of the structure. The added-mass effect occurs in the case for FSI1 and FSI3, where ${}^s\rho = {}^f\rho$. The added-mass effect is a numerical instability that occurs when the density of the structure is similar to or lower than the density of the fluid. FSI1, as it is a steady-state problems, does not cause significant stability issues, whereas FSI3 does. Therefore, subiterations need to be performed for FSI3, otherwise the solver would not converge. On the other hand, weak coupling is sufficient for FSI2.

In order to compare displacement of the structure, a reference point (point A) was chosen at the end of cantilever in the middle of its thickness. The displacement of the structure (at point A) for the FSI1, FSI2 and FSI3 benchmarks is shown in Table 2 and Figs. 2 and 3, respectively. FSI1 benchmark was performed with two different meshes, shown in Fig. 1, and different degrees of basis polynomials. The FSI2 and FSI3 benchmarks were performed with the finer mesh and cubic basis polynomials. An agreement with Turek and Hron benchmark in all the cases is indisputable. We can see that the y -component agrees better than the x -component, since the x -component of the amplitude is one order of magnitude lower than the y -component. A sequence of velocity fields during half a period is shown in Fig. 4 for FSI2 and FSI3 benchmarks.

Acknowledgements

The authors appreciate the kind support of the grant GA 20-26779S "Study of dynamic stall flutter instabilities and their consequences in turbomachinery application by mathematical, numerical and experimental methods" of the Czech Science Foundation and of the student grant project SGS-2019-009.

Table 2. FSI1 benchmark: x and y components of displacement at point A. Values $2.2708 \cdot 10^{-5}$ m and $8.2086 \cdot 10^{-4}$ m are considered exact x and y components of displacement, respectively

h [m]	elements	order	d_x [m]	d_x error [%]	d_y [m]	d_y error [%]
0.02	3040	2	$1.995 \cdot 10^{-5}$	12.2	$6.709 \cdot 10^{-4}$	18.3
0.02	3040	3	$2.221 \cdot 10^{-5}$	2.2	$7.568 \cdot 10^{-4}$	7.8
0.02	3040	4	$2.253 \cdot 10^{-5}$	0.8	$8.004 \cdot 10^{-4}$	2.5
0.01	12 092	2	$2.112 \cdot 10^{-5}$	7.0	$7.467 \cdot 10^{-4}$	9.0
0.01	12 092	3	$2.252 \cdot 10^{-5}$	0.8	$7.863 \cdot 10^{-4}$	4.2
0.01	12 092	4	$2.271 \cdot 10^{-5}$	0.0	$8.024 \cdot 10^{-4}$	2.3

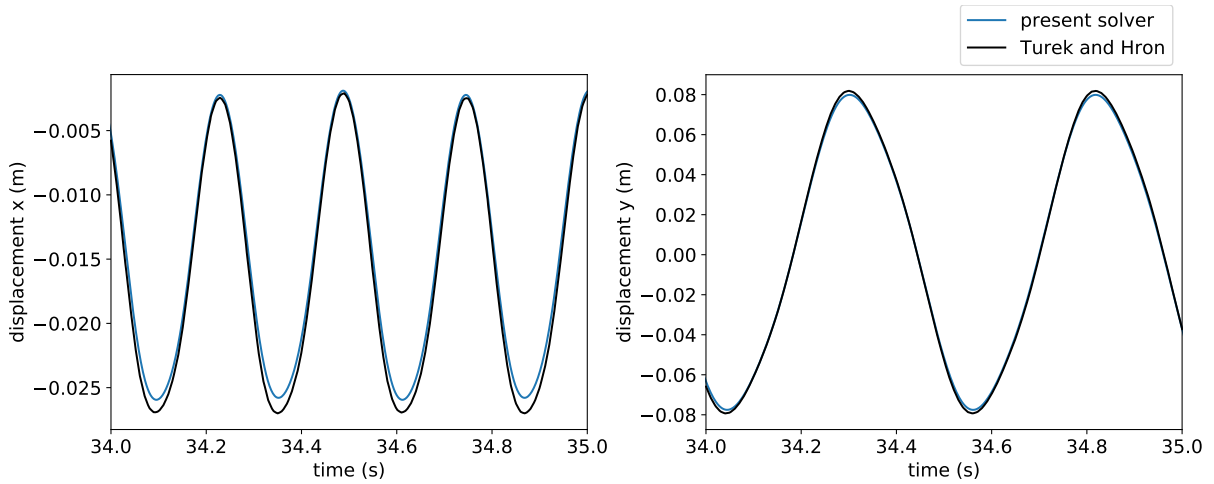


Fig. 2. FSI2 benchmark: displacement at point A

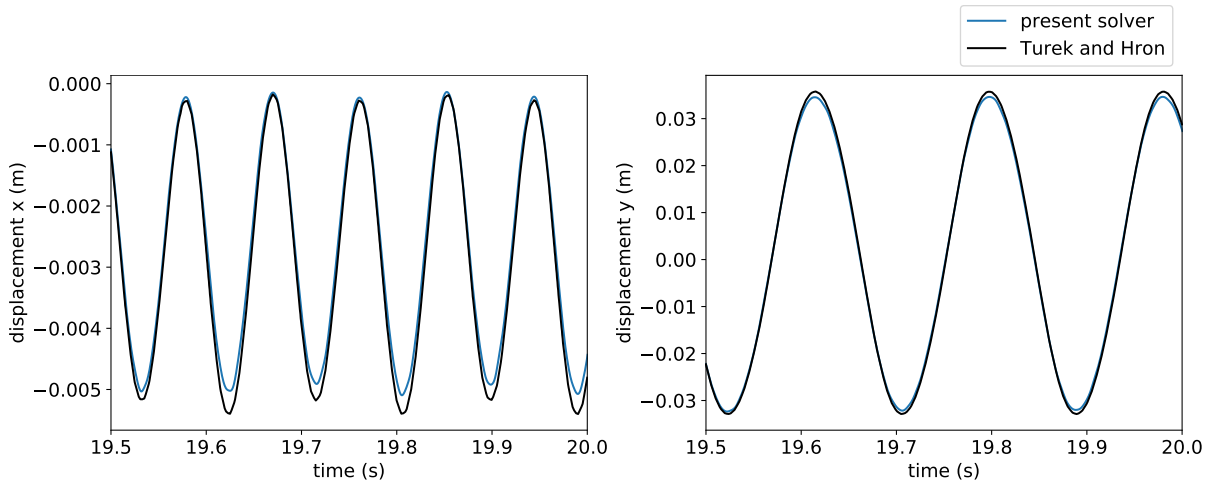


Fig. 3. FSI3 benchmark: displacement at point A

References

- [1] Ondřej, B., Pecka, A., FlowPro [Source code], 2018. <https://github.com/ondrabublik/FlowPro>
- [2] Turek, S., Hron, J., Proposal for numerical benchmarking of fluid-structure interaction between an elastic object and laminar incompressible flow. In: Fluid-Structure Interaction (edit.: H. J. Bungartz, M. Schäfer), Springer Berlin Heidelberg, 2006, pp. 371-385.

- [3] Turek, S., Hron, J., Mádlík, M., Razzaq, M., Wobker, H., Acker, J., Numerical simulation and benchmarking of a monolithic multigrid solver for fluid-structure interaction problems with application to hemodynamics, Lecture Notes in Computational Science and Engineering 73 (2010) 193-220.

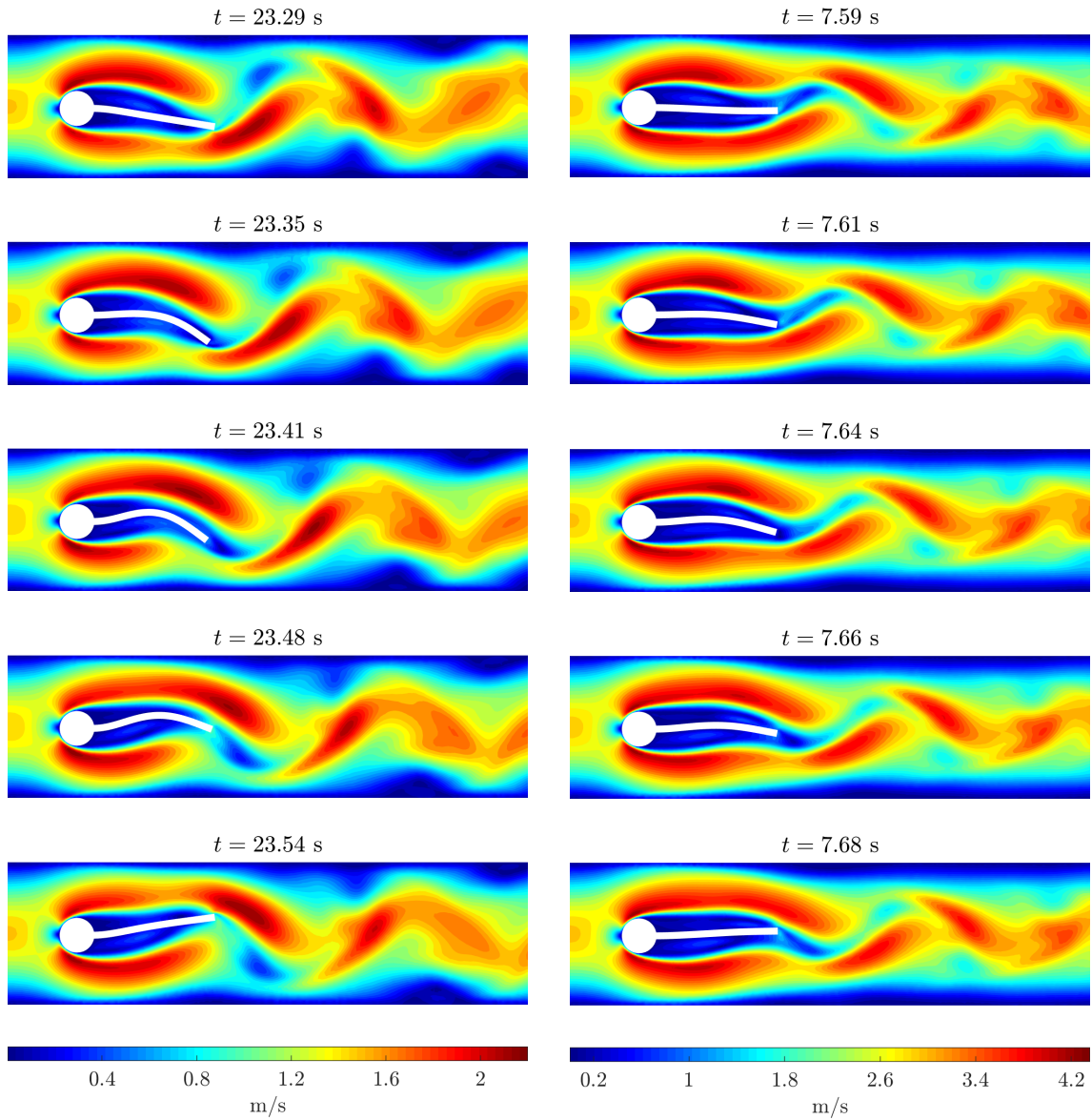


Fig. 4. Contours of velocity magnitude during half a period for the FSI2 (*left column*) and FSI3 (*right column*) benchmark